Advances in Geo-Energy Research

Vol. 2, No. 1, p. 1-13, 2018
www.astp-agr.com

Original article

# Permeability evaluation on oil-window shale based on hydraulic flow unit: A new approach

Pengfei Zhang[1,2], Shuangfang Lu[1*], Junqian Li[1*], Jie Zhang[1,2], Haitao Xue[1], Chen Chen[1,2]

[1]*Research Institute of Unconventional Oil & Gas and Renewable Energy, China University of Petroleum (East China), Qingdao 266580, P. R. China*

[2]*School of Geosciences, China University of Petroleum (East China), Qingdao 266580, P. R. China*

(Received December 18, 2017; revised January 3, 2018; accepted January 4, 2018; available online January 8, 2018)

**Citation:**
Zhang, P., Lu, S., Li, J., Zhang, J., Xue, H., Chen, C. Permeability evaluation on oil-window shale based on hydraulic flow unit: A new approach. *Advances in Geo-Energy Research*, 2018, 2(1): 1-13, doi: 10.26804/ager.2018.01.01.

**Corresponding author:**
*E-mail: lushuangfang@upc.edu.cn (S. Lu), lijunqian1987@126.com (J. Li)

**Keywords:**
Permeability
porosity
shale
hydraulic flow units
back propagation neural network

**Abstract:**
Permeability is one of the most important petrophysical properties of shale reservoirs, controlling the fluid flow from the shale matrix to artificial fracture networks, the production and ultimate recovery of shale oil/gas. Various methods have been used to measure this parameter in shales, but no method effectively estimates the permeability of all well intervals due to the complex and heterogeneous pore throat structure of shale. A hydraulic flow unit (HFU) is a correlatable and mappable zone within a reservoir, which is used to subdivide a reservoir into distinct layers based on hydraulic flow properties. From these units, correlations between permeability and porosity can be established. In this study, HFUs were identified and combined with a back propagation neural network to predict the permeability of shale reservoirs in the Dongying Depression, Bohai Bay Basin, China. Well data from three locations were used and subdivided into modeling and validation datasets. The modeling dataset was applied to identify HFUs in the study reservoirs and to train the back propagation neural network models to predict values of porosity and flow zone indicator ($FZI$). Next, a permeability prediction method was established, and its generalization capability was evaluated using the validation dataset. The results identified five HFUs in the shale reservoirs within the Dongying Depression. The correlation between porosity and permeability in each HFU is generally greater than the correlation between the two same variables in the overall core data. The permeability estimation method established in this study effectively and accurately predicts the permeability of shale reservoirs in both cored and un-cored wells. Predicted permeability curves effectively reveal favorable shale oil/gas seepage layers and thus are useful for the exploration and the development of hydrocarbon resources in the Dongying Depression.

## 1. Introduction

Due to developments in horizontal well and hydraulic fracturing techniques, shale has received renewed attention and has emerged as a commercial hydrocarbon reservoir. Numerous artificial fracture networks are generated within shale reservoirs after hydraulic fracturing. Permeability controls the fluid flow from the shale matrix to artificial fracture networks and greatly affects the production and ultimate recovery of shale oil/gas (Li et al., 2017). The permeability of shale reservoirs is more difficult to estimate than in conventional reservoirs because shale consists of a complex and heterogeneous porous medium that is rich in organic matter and clay minerals (Jarvie et al., 2007; Yu, 2012; Sidiq et al., 2017; Zhang et al., 2017).

Various techniques, such as experimental core analysis, have been proposed to measure permeability. These methods provide accurate values of permeability but do not demonstrate the reservoir heterogeneity because time and cost constraints prohibit drilling in all well intervals (Nooruddin and Hossain, 2012). However, commonly available well logs can provide continuous information along the well and offer a less-expensive method of measuring permeability. In recent years, several methods have been used to correlate core permeability with well logs, such as multivariate regression (Chen et al., 2015), artificial neural networks (Aminian and Ameri, 2005; Zhou et al., 2010; Tahmasebi and Hezarkhani, 2012), neuro-fuzzy systems (Saemi and Ahmadi, 2008; Aïfa et al., 2014) and Support Vector Machines (Baziar et al., 2014). These methods have been powerful tools for predicting the permeability of sandstone (tight), and carbonate rock reservoirs. However, shale permeability prediction by these methods from well logs is difficult and complex, because shale reservoirs are dominated by nanometer-scale pores, which results in the

https://doi.org/10.26804/ager.2018.01.01.

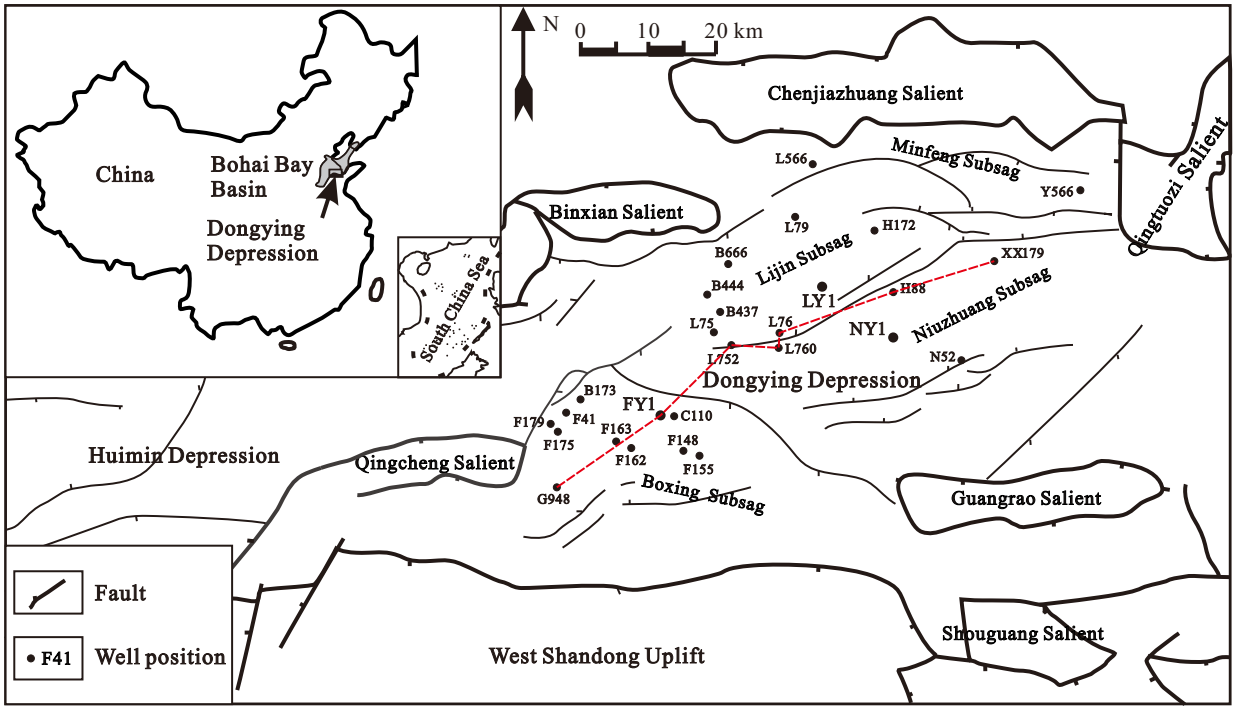


**Fig. 1.** Location and geological setting of the study area.

complex and heterogeneous pore fracture network (Nelson, 2009). Therefore, presenting a method, which can estimate the permeability of heterogeneous shales, is necessary.

A hydraulic flow unit (HFU) is a correlatable and mappable zone within a reservoir, in which fluid flow properties are uniform because of a similar pore throat structure (Hearn et al., 1984; Dou, 2000). Flow unit zonation subdivides a reservoir into layers based on hydraulic flow properties, thereby simplifying the heterogeneity. Each HFU is characterized by a flow zone indicator ($FZI$) and a strong correlation between permeability and porosity can be established (Amaefule et al., 1993). Moreover, porosity prediction from well logs is simpler than permeability prediction. Therefore, porosity can be used to estimate the permeability within each HFU based on a porosity-permeability transformation (Al-Ajmi and Holditch, 2000; Desouky, 2005; Jiao and Xu, 2006; Bhattacharya et al., 2008; Guo et al., 2010; Xiao et al., 2013; Orodu et al., 2016).

Multiple linear regression modeling using well log data has been the main method of estimating porosity in sandstone (tight), carbonate and volcanoclastic rock reservoirs (Zhang et al., 2012a; Zhang et al., 2016). However, petrophysical investigations suggest that the linear correlations between porosity and log data are indeterminate, particularly for tight shale reservoirs with complex mineral and fluid compositions (Lian et al., 2006). Back propagation (BP) neural networks have a flexible model structure that can be used to include non-linear, complex interactions between the model input and output. BP neural networks have been successfully employed to estimate porosity in heterogeneous petroleum reservoirs (Zhang, 2005; Ali and Ebrahim, 2016).

The objective of this paper is to predict the permeability of shale reservoirs in the Dongying Depression, Bohai Bay Basin using core and well log data from three wells (FY1, LY1 and NY1). The HFUs in the study reservoirs are based on core data, which are used to determine the $FZI$ and the porosity-permeability transformation for each HFU. The well logs are analyzed for well FY1 and LY1, and then correlated with core date information by BP neural network to produce reliable prediction models for porosity and $FZI$, respectively. The permeability estimation method is constructed with data from wells FY1 and NY1, and the generalization capability is verified by NY1 core data. The shale reservoir permeability values in un-cored wells are also estimated using this method. The results of this research have many applications for the exploration and development of shale oil/gas in the Dongying Depression.

## 2. Geological setting

The Dongying Depression is located in the southeastern portion of Bohai Bay Basin (Fig. 1) and is one of the most petroliferous depressions in China, spanning approximately 5800 km$^2$. It can be divided into four subsags ($i.e.$, Boxing, Lijin, Minfeng and Niuzhuang). According to the regional history and sedimentary sequences, the evolution of the Dongying Depression can be divided into syn-rift and post-rift stages (Xie et al., 2006). Dark shales (including mudstones and shales) are the main source rocks of the upper part of the fourth member (Es4$^U$) and of the lower part of the third member (Es3$^L$) in the Paleogene Shahejie Formation. Es4$^U$ and Es3$^L$ formed in a saline and a humid lacustrine environment, respectively, and were deposited during the syn-

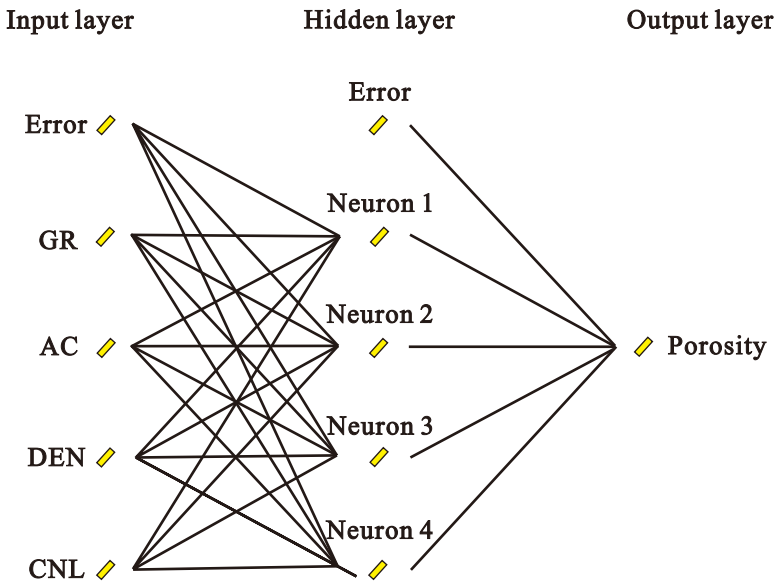


**Fig. 2.** Basic schematic of BP neural network.

rift stage. These two members have a high TOC content, as well as type I and $II_1$ maturity kerogen (0.42-0.64 $R_o\%$) and are the primary targets of shale oil/gas exploration in the study area (Zhang et al., 2012b; Zhang et al., 2014).

In this study, log information from three shale oil wells (FY1, LY1 and NY1) were used (Fig. 1). Wells FY1, LY1 and NY1 have 78, 24 and 21 data points, respectively. Modeling and validation datasets were constructed to assess the performance of the permeability estimation method. The modeling dataset consisted of 102 data points from wells FY1 and LY1, while the validation dataset included 21 data points from well NY1.

## 3. Methods

### 3.1 Hydraulic flow units

A hydraulic flow unit (HFU) is a reservoir unit in which fluid flow properties are uniform due to similar pore throat properties (Amaefule et al., 1993; Aguilera and Aguilera, 2001; Clarkson et al., 2012; Chen et al., 2016; Al-Rbeawi and Kadhim, 2017; Onuh et al., 2017). A hydraulic unit scheme was proposed to identify HFUs within a reservoir based on the modified Koseny-Carman equation and the mean hydraulic radius (Taghavi et al., 2007; Rahimpour-Bonab et al., 2012; Aguilera, 2014; Chen and Zhou, 2017). The Koseny-Carman equation expresses permeability as a function of effective porosity, shape factor, tortuosity and specific surface area. The equation is commonly expressed as follows (Carman, 1937):

$$k = \frac{1}{F_S \tau^2 S_{gv}^2} \frac{\varphi^3}{(1-\varphi)^2} \tag{1}$$

where $k$ is permeability in $\mu m^2$, $F_S$ is the shape factor, $\tau$ is the tortuosity, $S_{gv}$ is the specific surface area of the grain in $\mu m^{-1}$ and $\varphi$ is the effective porosity (fraction).

Rearranging and taking the square root of (Eq. 1) results in the following form:

$$0.0314\sqrt{\frac{k}{\varphi}} = \frac{1}{\sqrt{F_S}\tau S_{gv}} \frac{\varphi}{(1-\varphi)} \tag{2}$$

where the left hand side of (Eq. 2) is the reservoir quality index ($RQI$) and the permeability ($k$) is expressed in units of $10^{-3}$ $\mu m^2$. The first term on the right hand side is the flow zone indicator ($FZI$) and $\varphi/(1-\varphi)$ is the normalized porosity ($PMR$). Rearrangement of (Eq. 2) yields the following:

$$FZI = \frac{RQI}{PMR} \tag{3}$$

By taking the logarithm of (Eq. 3), the following relationship is derived:

$$lg(RQI) = lg(PMR) + lg(FZI) \tag{4}$$

Theoretically, plotting $RQI$ versus $PMR$ should yield a unit slope line on a log-log plot where reservoir samples with similar $FZI$ values lie in similar locations along this line. Samples with different $FZI$ values lie on adjacent parallel lines, with each having a distinct range of $FZI$ values. Using the cumulative plot of $lg(FZI)$, the optimal number of HFUs and their associated and $lg(FZI)$ intervals can be determined (Kadkhodaie-Ilkhchi et al., 2013). The porosity-permeability relationship on a semi-log plot can be defined for each HFU and subsequently used to estimate permeability.

### 3.2 Back propagation (BP) neural network

A Back Propagation (BP) neural network is a multilayer feed-forward artificial neural network (ANN) that uses an error back propagation algorithm for training. A BP neural network is a nonlinear dynamic system that processes large-scale, parallel-distributed information with variable structure,

high nonlinearity, and self-learning and self-organization characteristics (Wu et al., 2016).

A BP neural network consists of an input layer, one or more hidden layer(s) and an output layer (Hornik et al., 1989). A single hidden layer is common as additional hidden layers rarely improve the model (Baziar et al., 2014). Given a training set of input and output data, the back propagation algorithm divides the learning process into two stages (Fig. 2). In the forward propagation stage, the external input information is processed by the hidden layer to compute the output signal. In the error back propagation stage, if the output differs from the expected value, modifications to the connection weights are made in each layer based on the difference between the computed and the expected values, defined as the error. Discerning the optimal number of neurons in the hidden layer is a challenging step in BP neural network modeling (Nabipour and Keshavarz, 2017). A lower-than-optimum number of neurons in the network will result in incorrect training. Conversely, too many neurons in the network may cause overfitting, resulting in low precision (Hamzehie et al., 2015).

## 4. Results and discussion

### 4.1 Porosity and permeability of shale core samples

Porosity and permeability are considered the two most important parameters in hydrocarbon reservoir evaluation because they reflect the storage and flow capacities of a medium (Kadkhodaie-Ilkhchi et al., 2013; Li et al., 2017b). Fig. 3 shows the distributions and a cross plot of core porosity and permeability for three shale oil wells in the Dongying Depression. The porosity of shale samples varies from 2.4% to 19.5% (mean 7.83%). The majority of shale sample porosities range from 4% to 8% (Fig. 3(a)). Permeability values range from $0.024 \times 10^{-3}$ $\mu$m$^2$ to $10.4 \times 10^{-3}$ $\mu$m$^2$ with an average of $1.303 \times 10^{-3}$ $\mu$m$^2$. However, permeability values are less than $1 \times 10^{-3}$ $\mu$m$^2$ in 91 of the 123 shale samples, with the majority ranging from $0.01 \times 10^{-3}$ $\mu$m$^2$ to $0.5 \times 10^{-3}$ $\mu$m$^2$ (Fig. 3(b)). Moreover, the semi-log plot of the complete core dataset shows a poor correlation between permeability and porosity (Fig. 3(c)). Thus, the shale reservoirs within Es3$^L$ and Es4$^U$ typify low-porosity and low-permeability reservoirs.

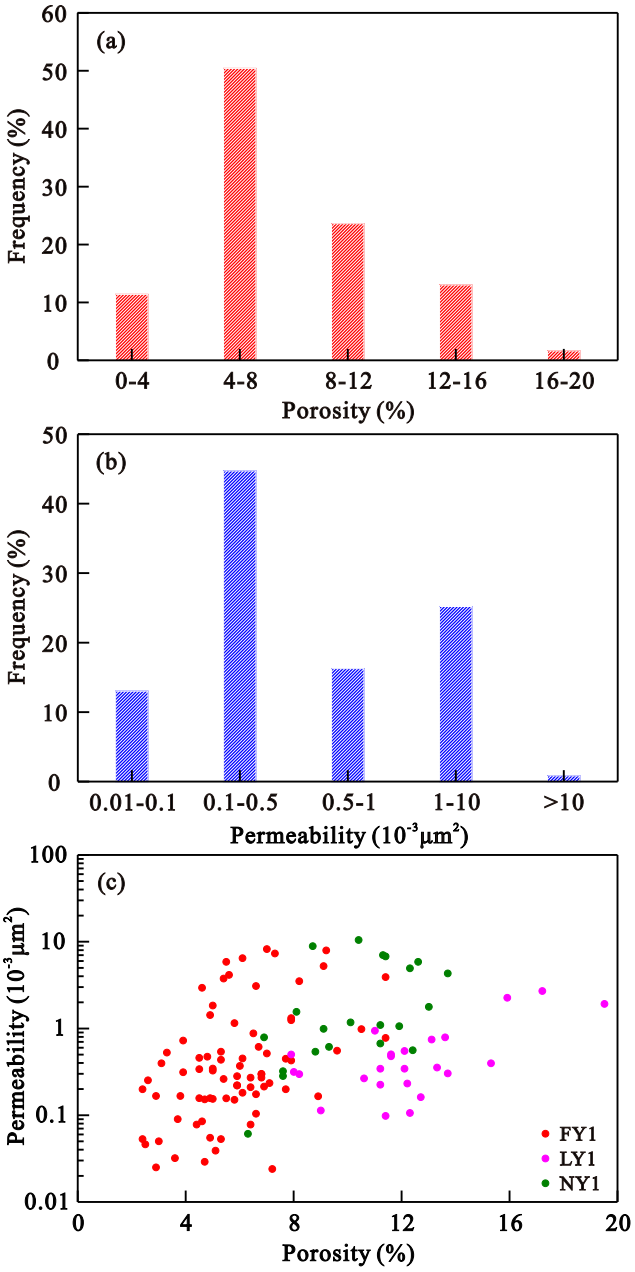


**Fig. 3.** Core porosity and permeability distributions in the Dongying Depression shale reservoirs.

### 4.2 Porosity estimation by BP neural network

Porosity is commonly determined by three types of well log data: sonic travel time (AC), bulk density (DEN) and neutron porosity (CNL). Total porosity is determined by well log data and is affected by the high clay content of shale reservoirs, while effective porosity is measured in the laboratory using well cores. Gamma ray logs (GR) can efficiently reveal clay content of the formations and can be used to control for the shale reservoir clay content. Therefore, in this study a BP neural network porosity model was established using three porosity and gamma ray logs as input vectors to output a core-based porosity scalar. To reduce the large differences parameter values, the logging data values were normalized to between 0 and 1.

The multilayer perceptron (MLP) neural network model in the SPSS Modeler 14.1 software was used to establish a BP neural network model to estimate porosity, consisting of input, hidden and output layers. The boosting model was employed to improve the BP neural network model accuracy. Termination of training was based on two criteria: minimum mean squared error and maximum training time. In this study, trial and error was used to find the appropriate network within the MLP architecture. Then, the modeling dataset was randomly divided into training and test subsets. To achieve the optimal structure, the proportion of data included from the training subset varied from 50% to 99%, while the proportion of the test subset data included varied from 50% to 1%. For each training and test

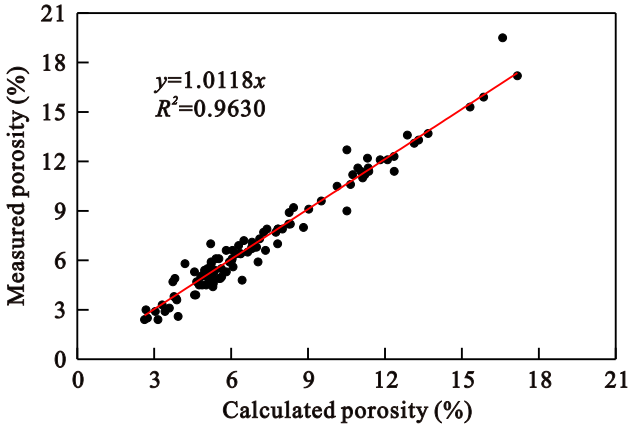


**Fig. 4.** Comparison of the calculated and measured porosities.

dataset, the optimal number of hidden layer neurons was automatically calculated by the software. The results indicate that the MLP architecture was optimal when the training and test subsets consisted of 79 and 23 data points, respectively. Moreover, a strong positive correlation ($R^2$ = 0.96) was observed between the calculated and measured porosities (Fig. 4).

## 4.3 HFU identification and prediction

### 4.3.1 HFU identification in shale core samples

Hydraulic flow units were determined using a modified Koseny-Carman equation based on the porosity and permeability of shale core samples (Tiab and Donaldson, 2012). Breaks in slope on the cumulative frequency plot of $lg(FZI)$ data were used to determine five HFU intervals in the shale core samples (Fig. 5(a), Table 1). The log-log plot of $RQI$ versus $PMR$ for the five HFUs is shown in Fig. 5(b). The $RQI$ and $PMR$ of each HFU lie in similar positions along a unit slope line, with the intercept representing the average $FZI$ value for each HFU. The semi-log plot of permeability and porosity shows the correlations between these two variables for all five HFUs (Fig. 5(c)). The correlation coefficient of each HFU is significantly greater than the correlation coefficient of the whole dataset (Fig. 3), indicating that the porosity and permeability of each HFU are distinct. Furthermore, two shale samples with similar porosities may have different values of permeability. This difference is due to the presence of pore structures dominated by sedimentary and diagenetic processes within each HFU (Kadkhodaie-Ilkhchi et al., 2013; Yarmohammadi et al., 2014). Therefore, porosity-permeability transformations can be used to estimate the permeability values of each HFU.

$RQI$ is the primary factor that controls reservoir quality and reflects the pore structure properties of porous media. The relationships between porosity, permeability and $RQI$ for the five HFUs are shown in Fig. 6. Permeability shows a stronger relationship with $RQI$ than with porosity, indicating that permeability is a key parameter in petroleum reservoirs,

**Table 1.** FZI intervals used for HFU identification.

| Hydraulic flow units | $lg(FZI)$ interval |
|---|---|
| HFU A | $0.4 \leq lg(FZI)$ |
| HFU B | $0.14 \leq lg(FZI) < 0.4$ |
| HFU C | $0.1 \leq lg(FZI) < 0.14$ |
| HFU D | $-0.4 \leq lg(FZI) < -0.1$ |
| HFU E | $lg(FZI) < -0.4$ |

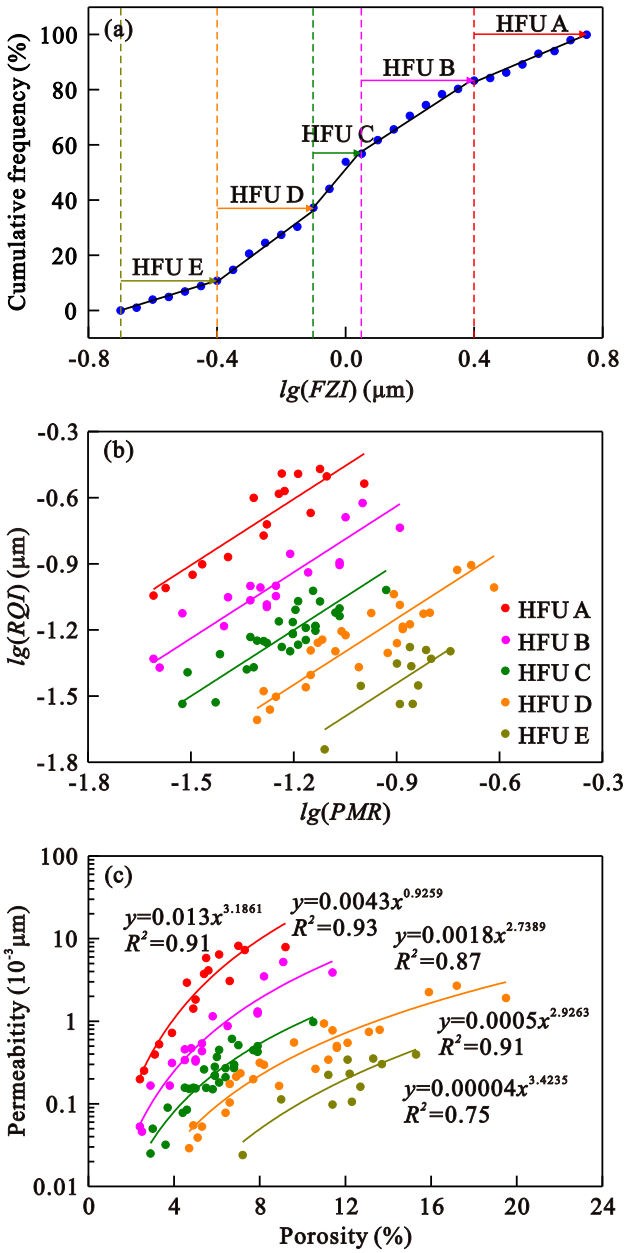


**Fig. 5.** Identification of the five HFUs and associated data, (a) cumulative frequency plot of $lg(FZI)$ data, (b) $RQI$-$PMR$ and (c) porosity-permeability.

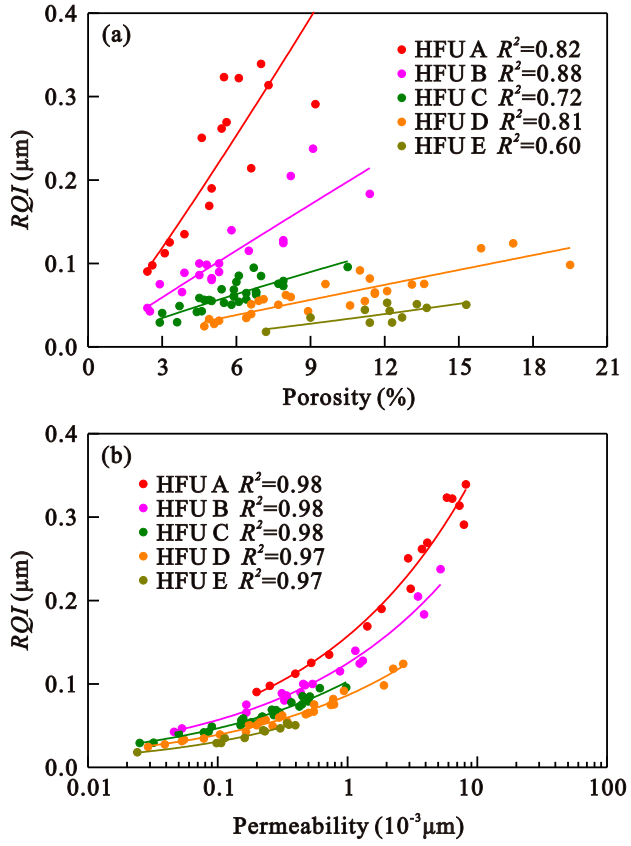


**Fig. 6.** Relationship between (a) porosity and $RQI$ and (b) permeability and $RQI$ for each HFU.

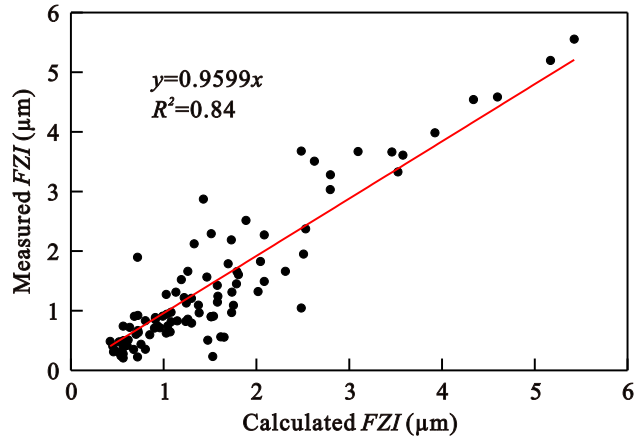


**Fig. 7.** Comparison of the calculated and measured $FZI$ values.

greatly affecting fluid seepage and production (Tahmasebi and Hezarkhani, 2012; Cao et al., 2016; Cronin et al., 2016).

### 4.3.2 FZI estimation and HFU prediction

The characterization of HFUs is based on the $FZI$ values calculated using porosity and permeability measurements of cored well rock samples. Normally, $FZI$ values from core samples are matched with corresponding well log data using various correlations, facilitating continuous HFU identification in both cored and un-cored wells. In this study, the correlations between $FZI$ values and well log data were modeled by a BP neural network. Compared to correlations with porosity, the correlations between $FZI$ values and well log data are difficult and complex. Therefore, a large number of well log data were selected using correlations with $FZI$ values, including caliper (CAL), spontaneous potential (SP), gamma ray (GR), neutron porosity (CNL), 4 m lateral resistivity (R4) and micro lateral resistivity (RLML) measurements. The $FZI$ BP neural network model was obtained by the same method used to generate the porosity model. The results demonstrated a strong positive correlation ($R^2$=0.84) between calculated and measured $FZI$ values when the training and test subsets consisted of 79 and 23 data points, respectively (Fig. 7). Thus, $FZI$ values estimated by this model can be used to identify HFUs in un-cored wells continuously (Table 1, Fig. 8 and 9).

### 4.3.3 Permeability estimation

Porosity-permeability transformations were obtained using the identified HFUs to estimate permeability. The exponential regression model has become popular for establishing porosity-permeability transformations and is advantageous because it uses a straight-line on a semi-log plot to discern the transformation. However, limited numbers of available datasets may result in high estimated permeability values for low porosity samples, and in particular, zero porosity cannot result in zero permeability (Jiao and Xu, 2006). Therefore, in this study, power function regression models were employed to determine the relationships between porosity and permeability (Jennings and Lucia, 2001), yielding high correlation coefficients (Fig. 5(c)). Using the permeability as the dependent variable in the power function model produced the following relationships in the study reservoirs (Fig. 5(c)):

HFU A: $k = 0.013\varphi^{3.1861}$, $R^2 = 0.9085$

HFU B: $k = 0.0043\varphi^{2.9254}$, $R^2 = 0.9259$

HFU C: $k = 0.0018\varphi^{2.7389}$, $R^2 = 0.8653$

HFU D: $k = 0.0005\varphi^{2.9263}$, $R^2 = 0.9080$

HFU E: $k = 4 \times 10^{-5}\varphi^{2.9263}$, $R^2 = 0.7482$

Using the five HFUs and their associated porosity-permeability transformations, continuous permeability values in wells FY1 and LY1 were predicted using the porosities estimated by the BP neural network model. Estimated permeability values correspond well to measured values, indicating that the model can accurately predict the permeability of shale reservoirs (Fig. 8 and 9).

## 4.4 Model validation and permeability estimation in un-cored wells

Models trained with the datasets from wells FY1 and LY1 were tested with data from well NY1 to assess their ability to estimate permeability in un-cored wells. Fig. 10 shows the predicted $FZI$, porosity and permeability values from well NY1 and reveals that the curves of these estimated parameters are similar to core-based value relationships. Therefore, the

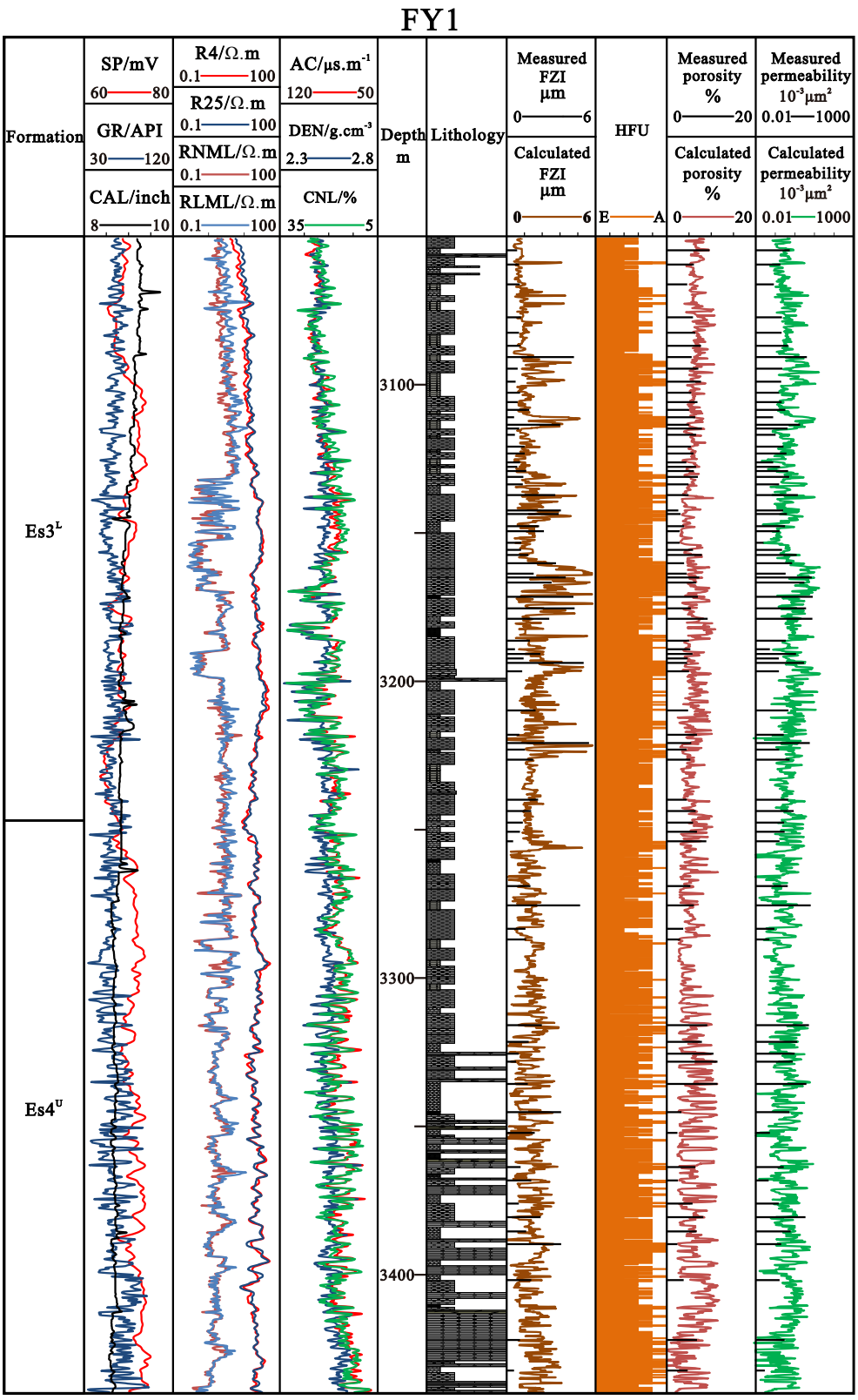


**Fig. 8.** HFU identification and estimated porosity and permeability values for wells FY1.

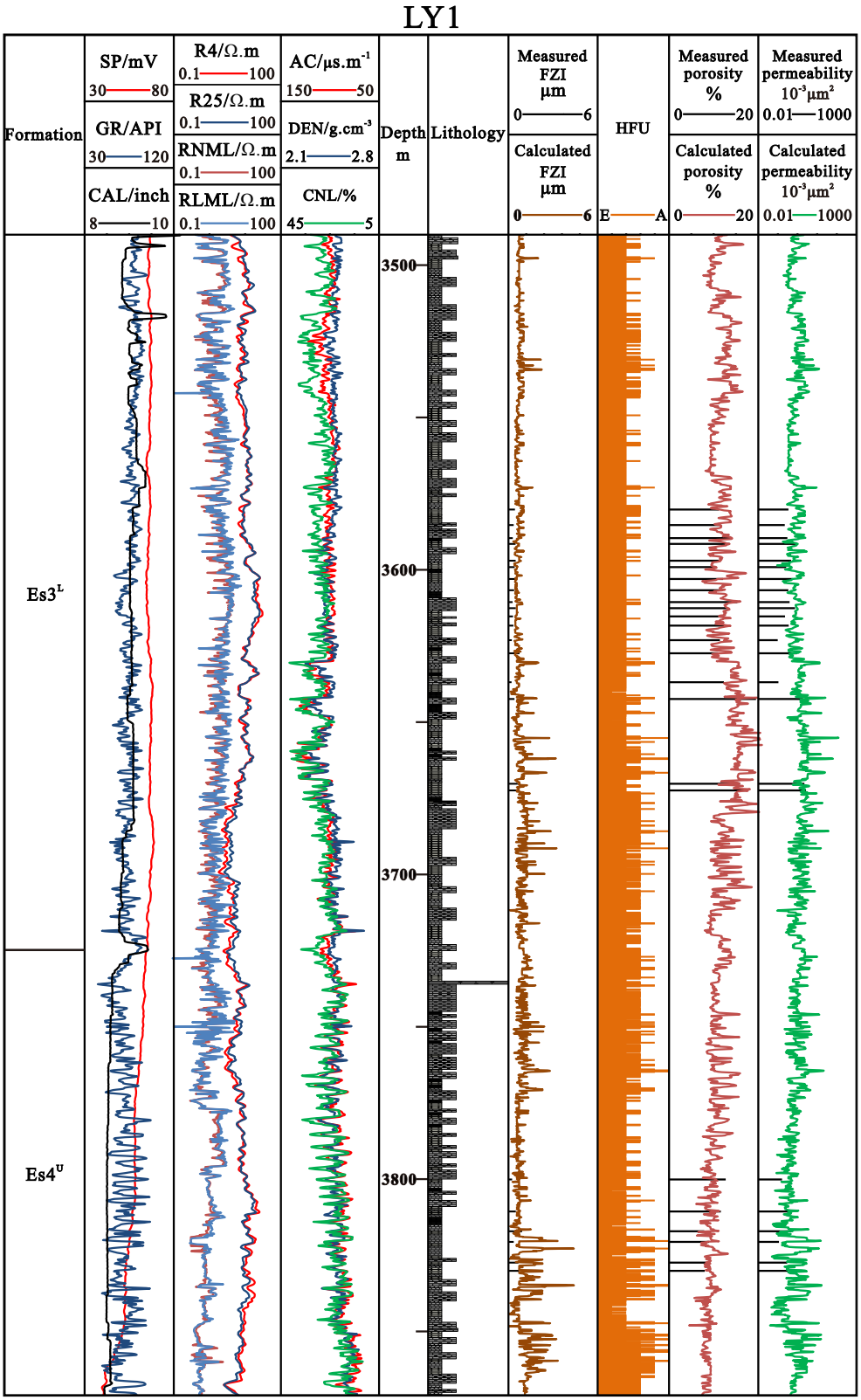


**Fig. 9.** HFU identification and estimated porosity and permeability values for wells LY1.

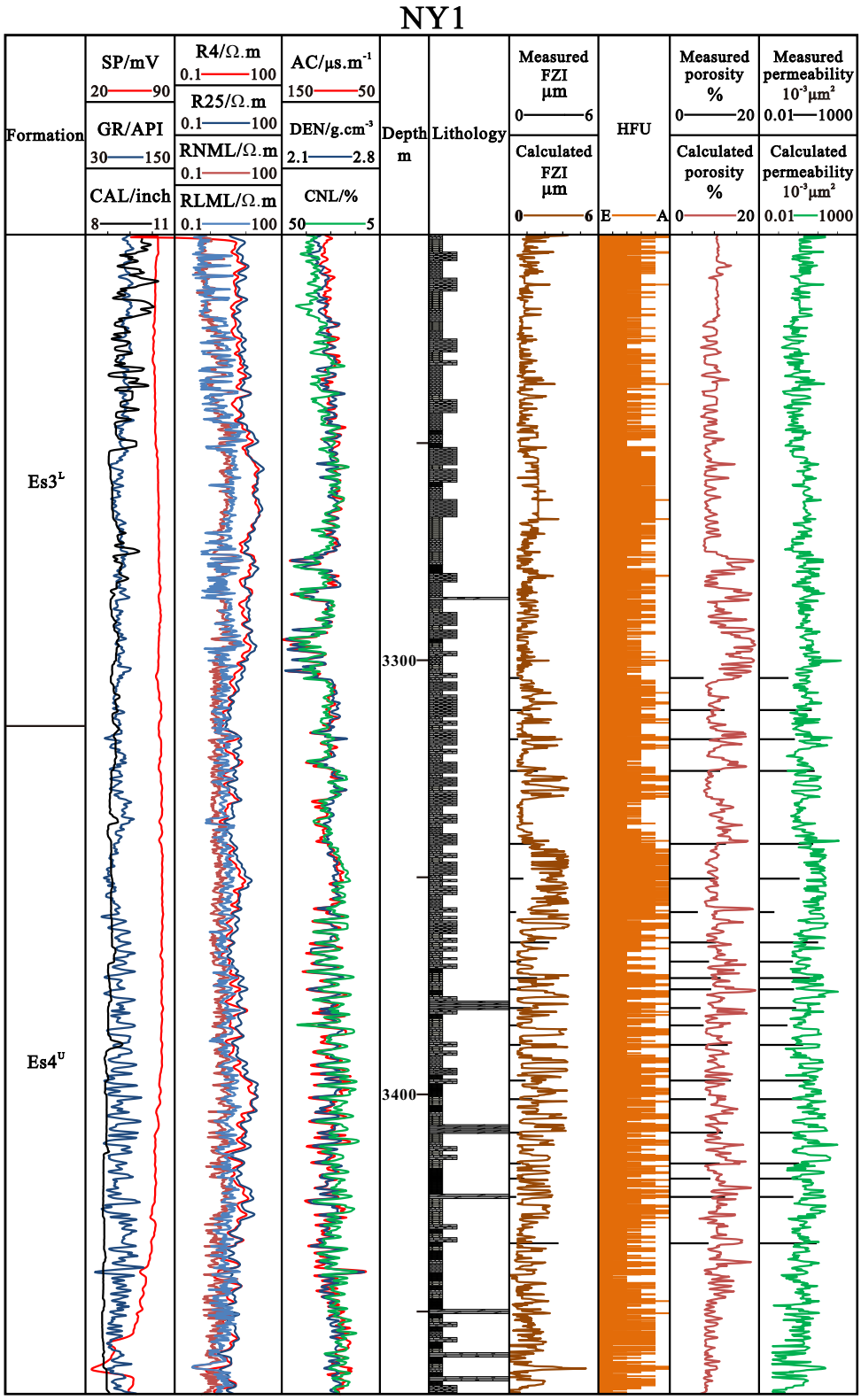


**Fig. 10.** HFU identification and estimated porosity and permeability values for well NY1.

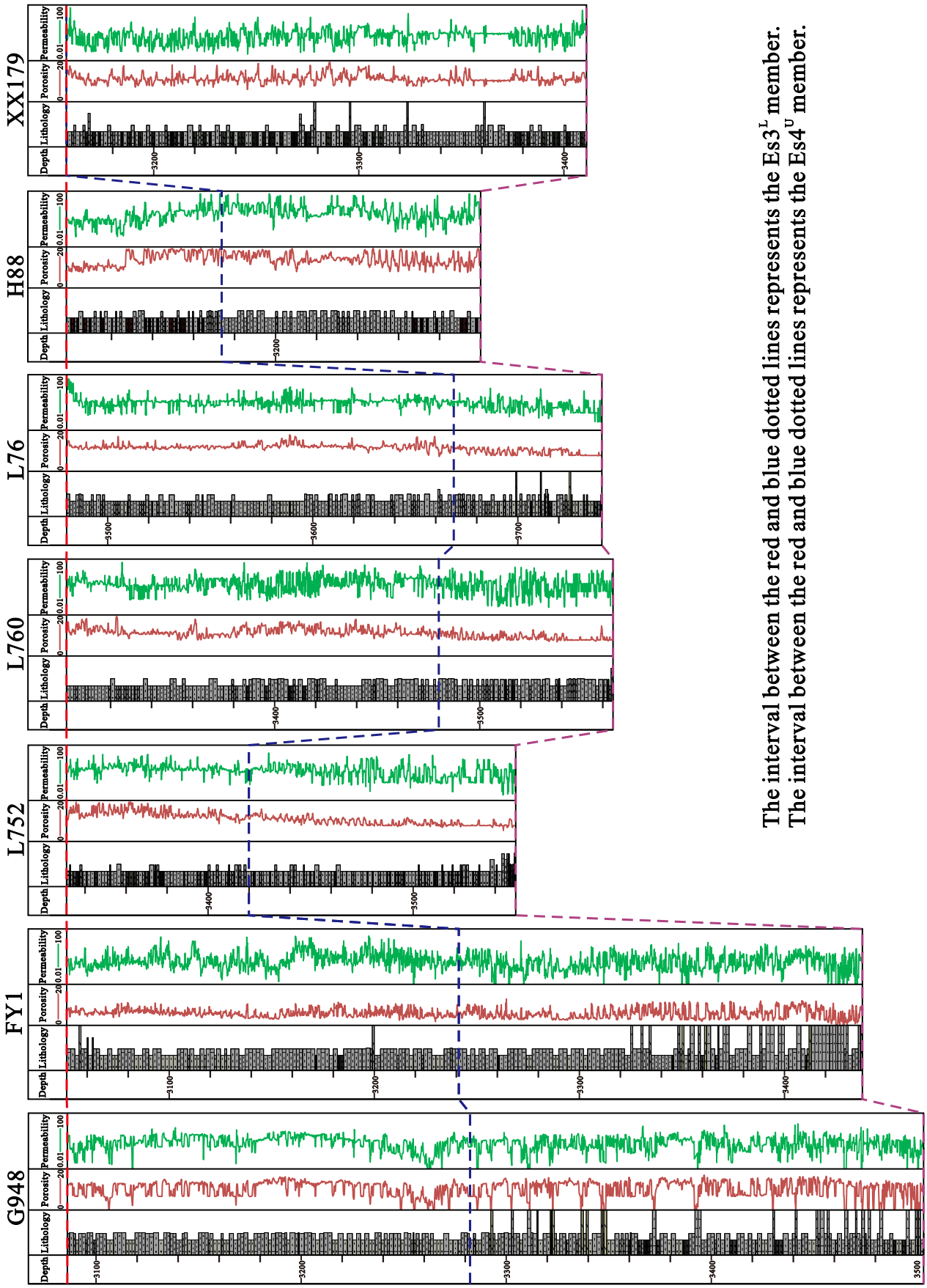


**Fig. 11.** Contrast plane in the calculate model.

models established using the training datasets can predict the permeability in un-cored wells. In this study, shale reservoir permeability was estimated in 24 un-cored wells within the Dongying Depression. Fig. 11 shows estimated permeability values for 7 wells. Furthermore, the predicted permeability curves effectively revealed favorable shale oil/gas seepage layers.

## 5. Conclusions

Using core porosity and permeability data along with statistical techniques, five hydraulic flow units were defined in shale reservoirs located within the Dongying Depression. In addition, porosity-permeability transformations with high correlations were established for each HFU.

Back Propagation neural network models were trained using the modeling datasets from wells FY1 and LY1 to predict porosity and $FZI$. By combining each HFU with a porosity-permeability transformation, a permeability estimation method was established to obtain continuous permeability in shale reservoirs. Estimated values of permeability correspond well to measured permeability values in wells FY1 and LY1.

The permeability estimation method, trained with data from wells FY1 and LY1, was tested with a core dataset from well NY1 to assess the method's ability to estimate permeability in un-cored wells. The results showed that the method can generate predicted permeability curves in un-cored wells, which effectively reveal favorable shale oil/gas seepage layers.

## Acknowledgments

This study was supported by the Key Program of the National Nature Science Foundation (41330313), the National Natural Science Foundation (41602131, 41572122, 41672130), and the Fundamental Research Funds for the Central Universities (17CX06036, 17CX02074, YCX2017002).



## References

Aïfa, T., Baouche, R., Baddari, K. Neuro-fuzzy system to predict permeability and porosity from well log data: A case study of Hassi RMel gas field, Algeria. J. Petrol. Sci. Eng. 2014, 123: 217-229.

Aguilera, R., Aguilera, M.S. The integration of capillary pressures and pickett plots for determination of flow units and reservoir containers. Paper SPE71725 Presented at the SPE Annual Technical Conference and Exhibition, New Orleans, Louisiana, 30 September-3 October, 2001.

Aguilera, R. Flow Units: From conventional to tight-gas to shale-gas to tight-oil to shale-oil reservoirs. SPE Reserv. Eval. Eng. 2014, 17(2): 190-208.

Al-Ajmi, F.A., Holditch, S.A. Permeability estimation using hydraulic flow units in a central arabia reservoir. Paper SPE63254 Presented at the SPE Annual Technical Conference and Exhibition, Dallas Texas, USA, 1-4 October, 2000.

Ali, D., Ebrahim, S. Physical properties modeling of reservoirs in Mansuri oil field, Zagros region, Iran. Petrol. Explor. Dev. 2016, 43(4): 611-615.

Al-Rbeawi, S., Kadhim, F. The impact of hydraulic flow unit & reservoir quality index on pressure profile and productivity index in multi-segments reservoirs. Petrol. 2017, 3(4): 414-430.

Amaefule, J.O., Altunbay, M., Tiab, D., et al. Enhanced Reservoir Description: Using core and log data to identify hydraulic (flow) units and predict permeability in uncored intervals/wells. Paper SPE26436 Presented at the SPE Annual Technical Conference and Exhibition, Houston, Texas, USA, 3-6 October, 1993.

Aminian, K., Ameri, S. Application of artificial neural networks for reservoir characterization with limited data. J. Petrol. Sci. Eng. 2005, 49(3): 212-222.

Baziar, S., Tadayoni, M., Nabi-Bidhendi, M., et al. Prediction of permeability in a tight gas reservoir by using three soft computing approaches: A comparative study. J. Nat. Gas Sci. Eng. 2014, 21: 718-724.

Bhattacharya, S., Byrnes, A.P., Watney, W.L., et al. Flow unit modeling and fine-scale predicted permeability validation in Atokan sandstones: norcan east Kansas. AAPG Bull. 2008, 92(6): 709-732.

Cao, C., Li, T., Shi, J., et al. A new approach for measuring the permeability of shale featuring adsorption and ultra-low permeability. J. Nat. Gas Sci. Eng. 2016, 30: 548-556.

Carman, P.C. Fluid flow through granular beds. Trans. Inst. Chem. Eng. 1937, 15: 150-166.

Chen, K.G., Chen, X., Zhang, J.H. Combined methods of permeability logging evaluate in glutenite reservoirs: A case study of Badaowan Formation in Karamay Oilfield. Adv. Earth Sci. 2015, 30(7): 773-779.

Chen, X.J., Yao, G.Q., Cai, J.C., et al. Fractal and multifractal analysis of different hydraulic flow units based on micro-CT images. J. Nat. Gas Sci. Eng. 2017, 48: 145-156.

Chen, X.J., Zhou, Y.F. Applications of digital core analysis and hydraulic flow units in petrophysical characterization. Adv. Geo-Energ. Res. 2017, 1(1): 18-30.

Clarkson, C.R., Jensen, J.L., Pedersen, P.K., et al. Innovative methods for flow-unit and pore-structure analyses in a tight siltstone and shale gas reservoir. AAPG Bull. 2012, 96(2): 355-374.

Cronin, M.B., Flemings, P.B., Bhandari, A.R. Dual-permeability microstratigraphy in the Barnett shale. J. Petrol. Sci. Eng. 2016, 142: 119-128.

Desouky, S.E.D.M. Predicting permeability in un-cored intervals/wells using hydraulic flow unit approach. J. Can. Petrol. Technol. 2005, 44(7): 55-58.

Dou, Z.L., Kaifa2000 S.K.Y. A study on flow unit model and distribution of remaining oil in fluvial sandstone reservoirs of the Guantao Formation in Gudong oil field. Petrol. Explor. Dev. 2000, 27(6): 50-52.

Guo, S.S., Cai, J., Zhou, J., et al. Hydraulic flow unit based permeability characterization and rapid production prediction workflow for an offshore field, South China Sea. Paper SPE131486 Presented at the International Oil and Gas Conference and Exhibition, Beijing, China, 8-10 June, 2010.

Hamzehie, M.E., Fattahi, M., Najibi, H., et al. Application of artificial neural networks for estimation of solubility of acid gases ($H_2S$ and $CO_2$) in 32 commonly ionic liquid and amine solutions. J. Nat. Gas Sci. Eng. 2015, 24: 106-114.

Hearn, C.L., Ebanks, W.J., Tye, R.S., et al. Geological factors Influencing reservoir performance of the hartzog draw field, Wyoming. J. Petrol. Technol. 1984, 36(8): 1335-1344.

Hornik, K., Stinchcombe, M., White, H. Multilayer feed-forward networks are universal approximators. Neural Networks 1989, 2(5): 359-366.

Jarvie, D.M., Hill, R.J., Ruble, T.E., et al. Unconventional shale-gas systems: the Mississippian Barnett Shale of north-central Texas as one model for thermogenic shale-gas assessment. AAPG Bull. 2007, 91(4): 475-499.

Jennings, J.W., Lucia, F.J. Predicting permeability from well logs in carbonates with a link to geology for interwell permeability mapping. Paper SPE71336 Presented at the SPE Annual Technical Conference and Exhibition, New Orleans, Louisiana, 30 September-3 October, 2001.

Jiao, C.H., Xu, C.H. An approach to permeability prediction based on flow zone index. Well Logging Technol. 2006, 30(4): 317-319.

Kadkhodaie-Ilkhchi, R., Rezaee, R., Moussavi-Harami, R., et al. Analysis of the reservoir electrofacies in the framework of hydraulic flow units in the Whicher Range Field, Perth Basin, Western Australia. J. Petrol. Sci. Eng. 2013, 111: 106-120.

Li, J.Q., Lu, S.F., Cai, Y.D., et al. Impact of coal ranks on dynamic gas flow: An experimental investigation. Fuel 2017a, 194: 17-26.

Li, J.Q., Yu, T., Liang, X., et al. Insights on the gas permeability change in porous shale. Adv. Geo-Energ. Res. 2017b, 1(2): 69-73.

Lian, C.B., Li, H.L., Qu, F., et al. Prediction of porosity based on BP artificial neural network with well logging data. Nat. Gas Geosci. 2006, 17(3): 382-384.

Nabipour, M., Keshavarz, P. Modeling surface tension of pure refrigerants using feed-forward back-propagation neural networks. Int. J. Refrig. 2017, 75(1): 217-227.

Nelson, P.H. Pore-throat sizes in sandstones, tight sandstones, and shales. AAPG Bull. 2009, 93(3): 329-340.

Nooruddin, H.A., Hossain, M.E. Modified Kozeny-Carmen correlation for enhanced hydraulic flow unit characterization. J. Petrol. Sci. Eng. 2011, 80(1): 107-115.

Onuh, H.M., David, O.O., Onuh, C.Y. Modified reservoir quality indicator methodology for improved hydraulic flow unit characterization using the normalized pore throat methodology (Niger delta field as case study). J. Petrol. Explor. Product. Technol. 2017, 7(2): 409-416.

Orodu, O.D., Tang, Z., Fei, Q. Hydraulic (Flow) Unit Determination and permeability prediction: A case study of block shen-95, Liaohe Oilfield, North-East China. J. Appl. Sci. 2009, 9(10): 1801-1816.

Rahimpour-Bonab, H., Mehrabi, H., Navidtalab, A., et al. Flow unit distribution and reservoir modelling in cretaceous carbonates of the sarvak formation, abteymour oilfield, dezful embayment, SW Iran. J. Petrol. Geol. 2012, 35(3): 213-236.

Saemi, M., Ahmadi, M. Integration of genetic algorithm and a coactive neurofuzzy inference system for permeability prediction from well logs data. Transport Porous Med. 2008, 71(3): 273-288.

Sidiq, H., Amin, R., Kennaird, T. The study of relative permeability and residual gas saturation at high pressures and high temperatures. Adv. Geo-Energ. Res. 2017, 1(1): 64-68.

Taghavi, A.A., M$\phi$rk, A., Kazemzadeh, E. Flow unit classification for geological modelling of a heterogeneous carbonate reservoir: cretaceous sarvak formation, dehluran field, SW Iran. J. Petrol. Geol. 2007, 30(2): 129-146.

Tahmasebi, P., Hezarkhani, A. A fast and independent architecture of artificial neural network for permeability prediction. J. Petrol. Sci. Eng. 2012, 86-87: 118-126.

Tiab, D., Donaldson, E.C. Petrophysics theory and practice of measuring reservoir rock and fluid transport properties. Oxford, United Kingdom: Elsevier Press, 2012.

Wu, B., Han, S.J., Xiao, J., et al. Error compensation based on BP neural network for airborne laser ranging. Opt. Int. J. Light Electron Optics 2016, 127(8): 4083-4088.

Xiao, L., Liu, X., Mao, Z.Q., et al. Tight-Gas-Sand Permeability Estimation From Nuclear-Magnetic-Resonance (NMR) Logs Based on the Hydraulic-Flow-Unit (HFU) Approach. J. Can. Petrol. Technol. 2013, 52(4): 306-314.

Xie, X.N., Fan, Z.H., Liu, X.F., et al. Geochemistry of formation water and its implication on overpressured fluid flow in the Dongying Depression of the Bohaiwan Basin, China. J. Geochem. Explor. 2006, 89(1-3): 432-435.

Yarmohammadi, S., Kadkhodaie-Ilkhchi, A., Rahimpour-Bonab, H., et al. Seismic reservoir characterization of a deep water sandstone reservoir using hydraulic and electrical flow units: A case study from the Shah Deniz gas field, the South Caspian Sea. J. Petrol. Sci. Eng. 2014, 118: 52-60.

Yu, B.S. Particularity of shale gas reservoir and its evaluation. Earth Sci. Front. 2012, 19(3): 252-258.

Zhang, L.P., Bai, G.P., Zhao, Y.Q. Data-processing and recognition of seepage and microseepage anomalies of acid-extractable hydrocarbons in the south slope of the Dongying depression, eastern China. Mar. Petrol. Geol. 2014, 57: 385-402.

Zhang, S.W., Zhang, L.Y., Li, Z., et al. Formation conditions of Paleogene shale oil and gas in Jiyang depression. Petrol. Geol. Recov. Effic. 2012b, 19(6): 1-5.

Zhang, Y.C., Liu, C., Fan, X.M. Application of multivariate regression analysis method in porosity calculation of

volcanic clastic rock. Global Geol. 2012a, 31(2): 377-382.

Zhang, Y.L. Porosity and permeability predictions in sand conglomerate reservoir from conventional well logs. Well Logging Technol. 2005, 29(3): 212-215.

Zhang, Z.J., Du, J.M., Zheng, Q., et al. The porosity interpretation model for the reservoir in Z area of Qaidam Basin. World Well Logging Technol. 2016, 211(1): 37-39.

Zhou, J.Y., Gui, B.W., Li, M., et al. An application of the artificial neural net dominated by lithology to permeability prediction. Acta Petrol. Sin. 2010, 31(6): 311-318.